INDIAN JOURNAL OF SCIENCE AND TECHNOLOGY

ORIGINAL ARTICLE

Energy Transfer Up-Conversion Effect on Characteristics of Nd^{+3}:YAG Passively Q-Switched Laser Pulse

Abdul-Kareem Mahdi Salih[1]*, **Asaad Hameed Jaafar**[1]

1 Physics department, College of Science, University of Thi-Qar, Iraq

OPEN ACCESS

Received: 19/04/2025

Accepted: 21/05/2025

Published: 29/06/2025

Citation: Mahdi Salih AK, Jaafar AH (2025) Energy Transfer Up-Conversion Effect on Characteristics of Nd^{+3}:YAG Passively Q-Switched Laser Pulse. Indian Journal of Science and Technology 18(25): 2031-2039. https://doi.org/10.17485/IJST/v18i25.745

* **Corresponding author**.

karimmahdisalih@yahoo.co.uk; Abdulkareem@Sci.utq.edu.iq

Funding: None

Competing Interests: None

Published By Indian Society for Education and Environment (iSee)

ISSN
Print: 0974-6846
Electronic: 0974-5645

Abstract

Objective: Energy transfer up-conversion effect on the characteristics of a passively Q-switched laser pulse has been investigated theoretically. **Method**: Rate equations model was proposed in this study. The model tested by numerical solving using Rung –Kutta- Fehelberg method in order to verify the validity of the physical and the mathematical hypotheses was used in the model through applying it to the passive Q-switching laser system consisting of Nd^{+3}:YAG as AM (quasi three-energy levels medium) with a Cr^{+3} : YAG crystal as a SA. The results of the proposed model show good agreement regarding the time behavior of the population inversion density and the photon density of the PQS pulse with the results of a previous theoretical study of the same system using rate equations not taking into consideration the effect of ETU. This benchmark enhances reliability using the model. **Findings**: The study indicated that the up-conversion processes caused a reduction in pulse energy and an increase in duration, resulting in a slight decrease in the pulse power. So, the pulse was generated at an earlier time in the case without up-conversion effect compared with the case with up-conversion effect. **Novelty**: The rate equation model has been modified, taking into account the. A model of rate equations was presented or proposed that took into account the calculation of the effect of energy transfer up-conversion processes in solid-state active media in passively Q-switched systems.

Keywords: Laser; Nd^{+3}: YAG; Q-switching passive; Q-switching; Energy transfer up-conversion

1 Introduction

Passively Q-switched (PQS) is one of the most famous methods used to obtain high-power laser pulses, which has a wide range of applications due to their characterizations, such as simple structure, low repetition rates, and small size, such as laser communication, high-precision processing, space detection, laser medical treatment, and radar [(1–4)]. Some nonlinear processes that occur in the active media (AM) of the PQS system may affect the characteristics of these high-power pulses to different degrees. One of these nonlinear processes is the energy transfer up-conversion (ETU). It is occur in high-doped solid-state laser active media, because of two ions interact in the excited state of AM, an interaction occurs between two excited ions in the excited laser level, and one of them gives part of its energy to the other ion, causing it to migrate to another higher energy level, while the ion that has lost part of its energy falls to a lower energy level in AM(5,6).

The topic of ETU phenomenon received the attention of researchers, such as in 2019, Pavel L. et al. presented their studies about ETU in Tm^{+3}: $LiYF_4$ Lasers at 2.3 μm(6). In 2020, S. Cante and J. I. Mackenzie, they presented their study about ETU in Nd^{+3}:YAG at cryogenic temperatures, when the crystal is cooled to liquid nitrogen temperature, despite a twofold increase in the macro parameter, it has a negligible effect on performance(7).

So, in 2020, Bo. Zhou et al. they are finding that the interfacial energy transfer (IET) an efficient approach for enabling photon up-conversion of lanthanide ions (e.g., Er^{+3}, Tm^{+3}, Ho^{+3}, Eu^{+3}, Tb^{+3}, Dy^{+3}, Sm^{+3}, and Nd^{+3})(8). In 2021, K. Mariselvam and Juncheng Liu presented a study in which they discussed the ETU in Er^{+3}/Tm^{+3}: MCZBP glasses(9).

In 2023, Y. LI et al. presented a study to determine the exact transmission of energy conversion coefficient for Er^{+3} and Yb^{+3} co-doped laser crystals. The results reveal that the ETU process in Er^{+3}, Yb^{+3}:YAB laser system is $5 \sim 35$ times stronger than that in Er^{+3} and Yb^{+3} co-doped phosphate glass(10).

Practically, the Z-scan technique is often used to estimate the effect of ETU in Nd^{+3}:YAG. This technique involves measuring the transmission of the pump laser through the Nd^{+3}: YAG crystal at different pump intensities(6).

In this study, we theoretically investigated the effect of ETU on PQS laser pulse characteristics, using another rare element in PQS optical system consisting of quasi three levels system of Nd^{+3}: YAG as AM and Cr^{+4}: YAG as a saturable absorbent material (SA) at room temperature. The absorption spectrum of Cr^{+4}: YAG is good and compatible with the emission spectrum of Nd^{+3}: YAG(11).

Nd^{+3}:YAG possesses a combination of properties uniquely favorable for laser operation, the YAG host is hard, good optical quality, and has a high thermal conductivity. Furthermore, the cubic structure of YAG favors a narrow fluorescent linewidth, which results in high gain and low threshold for laser operation(12).

The transition in Nd^{+3}:YAG occurs between the $^4F_{3/2}$ manifold to the $^4I_{11/2}$ manifold at 1064 nm, which the main laser, this transition represents four-level laser system. While the transition occurs between the $^4F_{3/2}$ manifold and the $^4I_{9/2}$ manifold at 946 nm, which represents quasi three- level laser system.

ETU processes in Nd^{+3}:YAG represents the energy migration process caused by the ions transfer from the excited laser level ($^4F_{3/2}$) to higher levels(5,9). Figure 1**(a,b)** shows the Nd^{+3}:YAG energy levels scheme and its up-conversion processes, respectively(13,14). While Figure 1 **-c** shows the energy levels diagram of Cr^{+4}: YAG(15).

2 Methodology

Based on rate equations model(16), a model of rate equations was presented or proposed in this study to investigate the effect of ETU on PQS pulse characteristics. In order to verify the validity of the physical and the mathematical hypotheses of the proposed model, this model is tested by numerical solving to investigate the PQS system, which consisting of Nd^{+3}: YAG as AM (quasi three- energy levels medium) with a Cr^{+3}: YAG crystal as an SA. The results of the proposed model were compared with regard to the time behavior of the population inversion density and the photons number density of the PQS pulse (φ) with the results of a previous theoretical study of the same system using rate equations not taken into consideration the effect of ETU(17). This benchmark enhances reliability using the model. After that, some studies were conducted, and their results were compared with the case of neglecting the effect of ETU and in the case of not neglecting it to determine the effect of ETU on the pulse characteristics.

3 Theory

The presented (suggested) rate equations model as the following:

$$\frac{d\varphi}{dt} = \varphi\left[K_{am}N - K_{sg}n_{sagl} - K_{se}n_{sael} - \gamma_c\right] \tag{1}$$

$$\frac{dN}{dt} = R_p - \gamma_p K_{am}N\varphi + \frac{N}{\tau_{am}} - WN^2 \tag{2}$$

$$\frac{dn_{sagl}}{dt} = -K_{sg}n_{sagl}\varphi + n_{sael}/\tau_{sae} \tag{3}$$

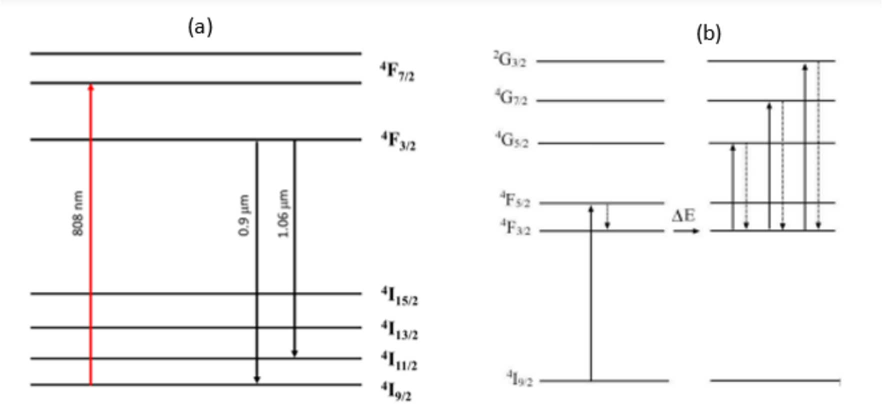

a: Nd^{+3}:YAG energy levels diagram [13])

b: Up-conversion processes in Nd^{+3}:YAG [14]

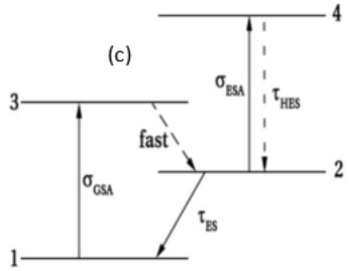

c: Cr^{+4}:YAG energy levels diagram [15]

Fig 1

$$\frac{dn_{sael}}{dt} = K_{sg} n_{sagl} \varphi - n_{asel}/\tau_{sae} \tag{4}$$

Where **Eq.1** represent the time variation of the laser photons density of PQS pulse $(\varphi)(cm^{-3})$. While **Eq.2** represent the time variation of population inversion density of ions (N) in AM (cm^{-3}), the fourth term in this **Eq. 2** represent the novelty of the model. **Eq.3** and **Eq.4** represent the time variation of ions population (ions number density) of the saturable absorbent ground level (SAGL) and saturable absorbent excited level (SAEL) (n$_{sagl}$, n$_{sael}$) respectively. $K_{am} = \frac{2\sigma_a l_{am}}{\tau_r}$ is the coupling coefficient between φ and N. σ_a is the emission cross sections (cm^2) of AM excited energy level, l_{am} is the AM length. $\tau_r = \frac{2l_c}{c}$ is the round trip transit time, l_c is the length of the cavity, c is the speed of light in vacuum. $K_{sg} = \frac{2\sigma_{sg} l_s}{\tau_r}$ is the coupling coefficient between φ and n$_{sagl}$, σ_{sg} is the absorption cross sections (cm^2) of n$_{sagl}$, l_s is the length of SA. $K_{se} = \frac{2\sigma_{se} l_s}{\tau_r}$ is the coupling coefficient between φ and n$_{sael}$, σ_{se} is the absorption cross sections (cm^2) of n_{asel}. $\gamma_c = \left(\ln\frac{1}{R} + L\right)$ is the decay rate of the cavity represents the all the losses in φ. $R = \sqrt{R_1 R_2}$, where R_1, R_2 are represent the reflectivity of rear mirror and output coupler mirror respectively, L is the photons lost due to absorbing and scattering mechanisms in the cavity. R_p is the pumping rate, γ_p is the reduction factor of population, which is equal to 1,2 for 4-levels, 3-levels systems of AM respectively, τ_{am} is the fluorescence lifetime of laser level in AM, τ_{sae} is the lifetime of SAEL, W is the up-conversion rate parameter. R_p and τ_{am} generally very long in time comparing with the generation time of PQS laser pulse(18), then the first term and the third term in Equ.2 can be neglect. So τ_{sae} is very long compared the generation of PQS laser pulse(19,20), then it is possible to neglect the second term of **Eq. 3 and Eq.4**, and rewrite these equations as following:

$$\frac{dN}{dt} = -\gamma_p K_{am} N \varphi - W\,N^2 \tag{5}$$

$$\frac{dn_{sagl}}{dt} = -K_{sg} n_{sagl} \varphi \tag{6}$$

$$\frac{dn_{sael}}{dt} = K_{sg} n_{sagl} \varphi \tag{7}$$

The initial value of the population inversion density (N_i) between the spectral lines of the AM can be estimated at the initial time by means of boundary conditions as follows $n_{sagl} \approx n_i$ or $n_{sael} \approx 0$, where ($n_i = n_{sagl} + n_{sael}$) is the total ions of SA, in **Eq.1** can be regards $\frac{d\varphi}{dt} \approx 0$ because of φ is very low in value at initial time , then the N_i value can be estimated by **Eq. 1** as the following:

$$N_i = \frac{K_{sagl}\, n_i + \gamma_c}{K_{am}} \tag{8}$$

At maximum photons density, the most of SA ions in SAEL, then can be regards $n_{sae}l \approx n_i (n_{sagl} \approx 0)$, so can be considering $\frac{d\varphi}{dt} \approx 0$. Then the threshold population inversion (N_t) can be estimated as the following:

$$N_t = \frac{K_{sael} n_i + \gamma_c}{K_{am}} \tag{9}$$

The energy of PQS pulse can be calculated by the expression (21):

$$E = \frac{(N_i - N_f)}{N_i} \frac{(N_i - N_f)\, hv}{\gamma_p} \tag{10}$$

Where N_f is the final population inversion density, can be obtained from computations. The pulse power can be estimated as the expression:

$$P = \frac{E}{\tau} \tag{11}$$

Where τ is the pulse duration, can be estimated by calculate the rising time and the falling time at the width of half maximum amplitude of pulse.

4 Results and Discussion

One of the important steps that must be taken before starting to conduct studies in this work is the verify the reliability of the mathematical model proposed in the study. The model has been tested by numerical solving using Rung-Kutta- Fehelberg method to investigates the PQS laser system consisting of Nd^{+3}:YAG as AM (quasi three-energy levels medium) with a Cr^{+3} : YAG crystal as a SA. The input data has been used in computation reported in Table 1 **-a**.

Figure 2**-a** represents the results from computations that did not neglect the ETU effect using the rate equations model presented in this paper. While Figure 2 **-b** represents a previous theoretical study in the PQS system involved same AM and SA (17), but it was not taken into consideration the ETU effect. When comparing the two figures, the time-varying behavior of both the population inversion density and photon density can be found to be very similar, but there was a slight difference in the values for specific time intervals.

Figure 3 shows the profile of PQS pulse behavior in terms with or without ETU processes effect. It appears that the pulse generated at earlier time in the case without ETU effect than with ETU effect. The pulses were generated at the time (57, 60 ns) approximately without and with ETU effect respectively. The maximum value of $\varphi(\varphi_{max.})$ increases in the case of without ETU effect, where its value was $\varphi_{max.} = 6.2961 \times 10^{17}$, while $\varphi_{max.} = 5.8919 \times 10^{17}$ in the case with effect of ETU processes. The study explains that; the energy which released as photons was decreased under the effect of ETU process; because of two reasons, the first is the decrease in the N_i, and the second is the increase in N_f as shown in Table 1 **-b**. Figure 4 shows the temporal behavior of the N as a function of ETU, where the N_i is slightly lower at with ETU processes effect compared with the case without the ETU processes due to the transfer of ions from the higher laser level to another energy levels not involved

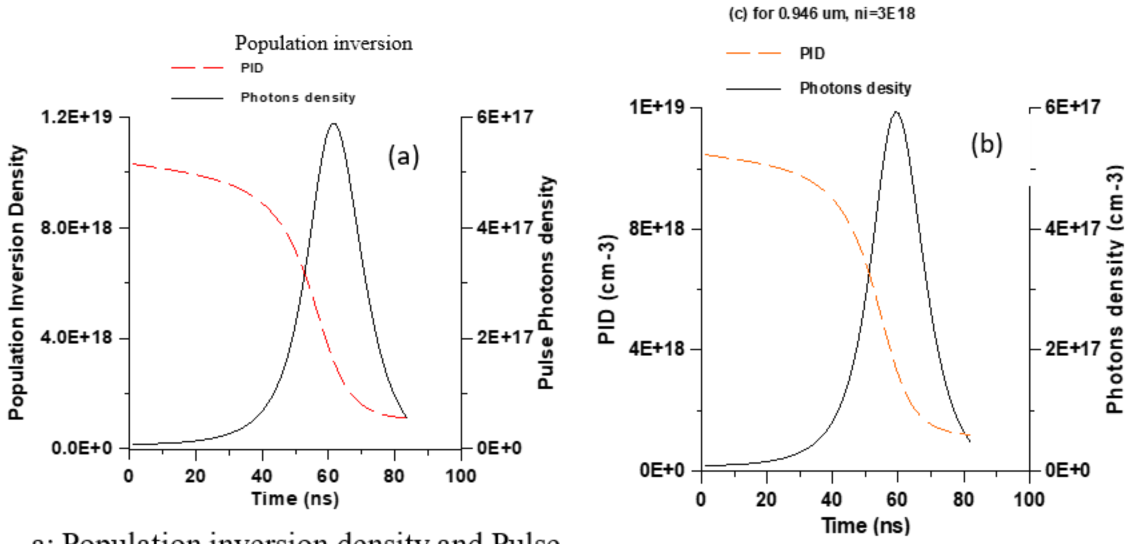

a: Population inversion density and Pulse photons density behavior with ETU using the presented model

b: Population inversion density (PID) and Pulse photons density without ETU [17]

Fig 2

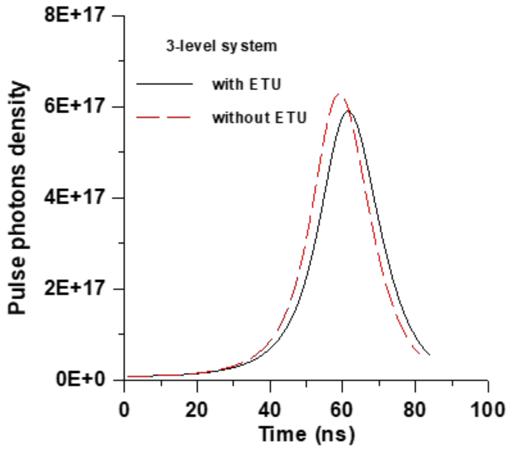

Fig 3. Photons density(cm^{-3}) of PQS pulse as a function of ETU

in the population inversion, and vice versa for the value of N_f as shown in Table 1 -**b**. Also Figure 4 shows that the temporal variation of the N of the two study cases with and without ETU effect is very close until about 38 ns, and then there is a clear variation through the interval time 38 ns to 84 ns approximately.

Figure 5 shows the behavior profile of the SAGL population is compared to ETU, it appears a significant convergence in the population value at the initial time of laser pulse generation until about 37 ns. This means that the effect of the presence of ETU processes is very small during this time period. The variation in the SAGL population values begins after the 37ns time instant. The study explains this by referring to Figure 3, can be noted that the variation in the value φ occurs at the 37 ns time instant. The decrease in φ under the influence of ETU, as shown in Figure 3, led to a decrease in the intensity of the interaction between φ and ions of SAGL.

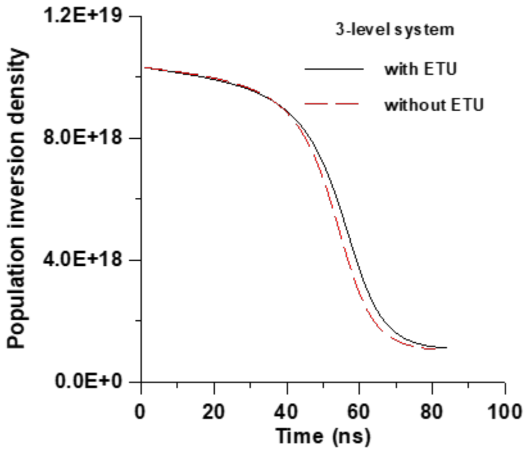

Fig 4. Population inversion density (cm^{-3}) as a function of ETU

This resulted in the level's population being higher than its population when the effect of ETU was not considered. It was also observed that at a time of about 80 ns. The effect is not significant, and the level's population converges regardless of the ETU's state.

Figure 6 shows the temporal behavior of the SAEL population in terms of ETU, it is depicted as a significant convergence in the population value at the initial time of laser pulse generation until approximately 37 ns. The effect of ETU processes is very small during this time period, but after that, there will be a change in population values. By referring to Figure 3, the study explains that the value of the φ in terms of ETU changes around the 37 ns instant. Without ETU's influence, the increase in φ at led to an increase in the intensity of the interaction between φ and the ions of the SAGL, which resulted in the transfer of ions to the irritated level in the SA, resulting in an increase in its population, and it is also noticeable that at about 75 ns, the effect of ETU is very small and the population of SAEL converges regardless of the with and without ETU processes.

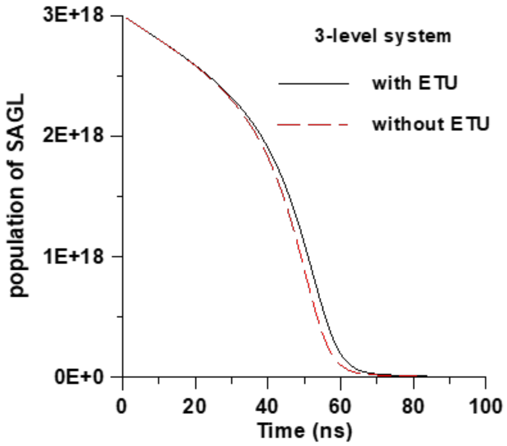

Fig 5. population of SAGL (cm^{-3}) as a function of ETU

Figure 7 illustrates the photon loss caused by the system cavity in terms of ETU processes, which has been observed to be constant over time in both cases with and without these processes. The study explains that the photon loss is not influenced by the AM spectrum and transitions, but rather by the effects of reflection, interference, diffraction, and scattering that are caused by mirrors and other physical components of the system cavity. However, this loss is a fraction of the total photon loss shown in Figure 8, in addition Figure 8 shows that the effect of ETU processes is evident in the time interval 37-75 ns, where the value of the photon loss rate is higher than when these processes are neglected for the same time instant. The study's explanation for this is based on the temporal behavior of the population inversion density as depicted in Figure 4.

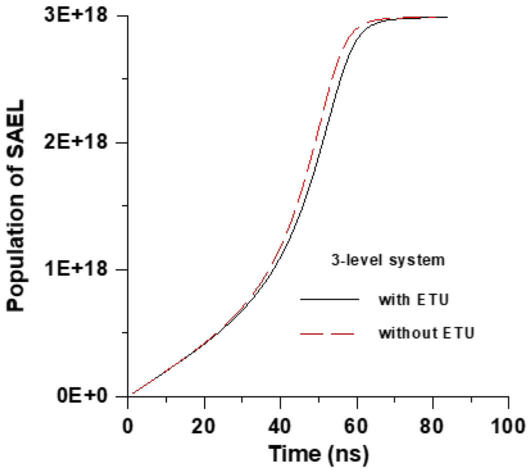

Fig 6. population of SAEL (cm^{-3}) as a function of ETU

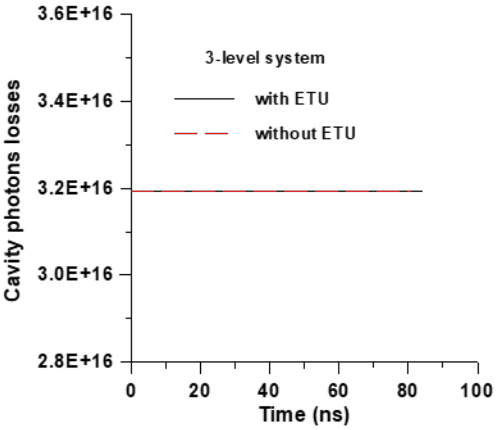

Fig 7. Cavity photons losses (cm^{-3}) as a function of ETU

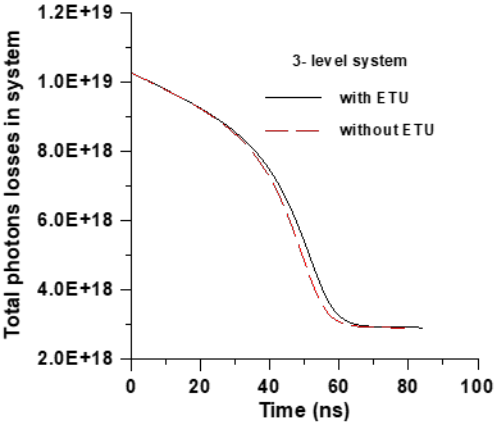

Fig 8. Total photons losses in system (cm^{-3}) as a function of ETU

The results show that ETU operations result in a slight decrease in pulse energy and an increase in pulse duration due to the slow buildup of the pulse, resulting in an increased rise time. Table 1 **-c** illustrates a decrease in pulse power as a result of the decrease in energy and duration.

Table 1

a: Input data of parameters

Param.	**Value**	**Refer.**	**Param.**	**Value**	**Refer.**
σ_a	$5.1\times10^{-20}\text{cm}^2$	(10)	λ	0.946um	(22)
σ_{sg}	$4\times10^{-18}\text{cm}^2$	(10)	γ_p	2	(23)
σ_{se}	$1.1\times10^{-18}\text{cm}^2$	(24)	W	$2.8\times10^{-22}\text{m}^3\text{s}^{-1}$	(10)
n_i	$3\times10^{18}\text{cm}^{-3}$		R_1	99%	
L	0.02		R_2	90%	
$\boldsymbol{l_s}$	0.35 cm		l_a	8 cm	

b: Values results of the essentials parameter of PQS pulse as a function of ETU

ETU	$\varphi_{max.}$ ***(cm^{-3})***	N_i ***(cm^{-3})***	N_{th} ***(cm^{-3})***	N_f ***(cm^{-3})***	N_{def} ***(cm^{-3})***
With ETU	5.892 x10^{17}	1.031 x10^{18}	3.044 x10^{18}	1.097 x10^{17}	9.229X10^{18}
Without ETU	6.3 x10^{17}	1.033x10^{18}	3.21 x10^{18}	1.052 x10^{17}	9.273 x10^{18}

C: Characteristics of PQS pulse as a function of ETU

ETU	**Raising time *(ns)***	**Falling time *(ns)***	**Duration *(ns)***	**Energy *(J)***	**Power *(w)***
With ETU	9.835	9.457	19.292	0.8664	4.491 x10^{7}
Without ETU	8.848	9.731	18.58	0.875	4.709x10^{7}

5 Conclusions

The mathematical model of the rate equations presented by the study can be used to study or investigate the effect of the ETU on the characteristics of the PQS laser high power pulses.

The up-conversion operations in Nd^{+3}: YAG as active medium of passive Q-switching lead to decrease the pulse energy and an increase in pulse duration, in result the slight reduces in pulse power. To avoid this loss in the pulse power, even if it is slight, it is necessary to increase the concentration of ions of the AM and avoid high temperature of the AM.

In cases with an up-conversion effect, the pulse generation occurs at delay short time compared without the up-conversion case.

References

1) Zeng K, Wu X, Jiang F, Zhang J, Kong J, Shen J, et al. Experimental research on micro hole drilling of polycrystalline Nd:YAG. *Ceramics International*. 2021. https://doi.org/10.1016/j.ceramint.2021.12.165.
2) Wang J, Xie L, Wang Y, Lan Y, Wu P, Lv J, et al. High-damage vanadium pentoxide film saturable absorbent for sub-nanosecond Nd:YAG lasers. *Infrared Physics & Technology*. 2023;p. 104580. https://doi.org/10.1016/j.infrared.2023.104580.
3) Hussein ZA, Salih AKM. A theoretical study of the output coupler reflectivity effect on the characteristics of Er+3 laser pulse at passively q-switching. *Edelweiss Applied Science and Technology*. 2024;8(6):4089–4100. https://doi.org/10.55214/25768484.v8i6.2899.
4) Hussein DS, Salih AKM. Study of Active Medium Length Effect on Characteristics of Passive Q-Switching and Stokes with Anti-Stokes Pulse. *Indian Journal of Science and Technology*. 2024;17(8):723–731. https://doi.org/10.17485/IJST/v17i8.2823.
5) Bergstrand J, Liu Q, Huang B, Peng X, Würth C, Resch-Genger U, et al. On the decay time of upconversion luminescence. *Nanoscale*. 2019;11:4959. https://doi.org/10.1039/c8nr10332.
6) Loiko P, Soulard R, Guillemot L, Brasse G, Doualan JL, Braud A, et al. Efficient Tm:LiYF4 Lasers at 2.3 μm: Effect of Energy-Transfer Upconversion. *IEEE Journal of Quantum Electronics*. 2019. https://doi.org/10.1109/JQE.2019.2943477.
7) Cante S, Mackenzie JI. Energy transfer upconversion in Nd:YAG at cryogenic temperatures. *Optical Materials Express*. 2020;10(9). https://doi.org/10.1364/OME.397034.
8) Li Q, Yan L, Zhang Q, Zhou B. Controlling upconversion through interfacial energy transfer (IET): fundamentals and applications. *Journal of Rare Earths*. 2020. https://doi.org/10.1016/j.jre.2020.01.009.
9) Mariselvam K, Liu J. Up-conversion, energy transfer and CIE analysis of Er3+/Tm3+: MCZBP glasses. *Optik*. 2021;242:167324. https://doi.org/10.1016/j.ijleo.2021.167324.
10) Li Y, Liu K, Feng J, Chen Y, Huang Y, Zhang K. Precise determination of energy transfer upconversion coefficient for the erbium and ytterbium codoped laser crystals. *Optics Express*. 2023;31(26). https://doi.org/10.1364/OE.509271.

11) Hussein DS, Salih AKM, Asal R. Investigation of Saturable Absorbent Length Effect on Characteristics of Passive Q-Switching and Stokes with Anti-Stokes Pulses Generated in Laser System of Nd:YVO4. *University of Thi-Qar Journal of Science (UTJsci)*. 2024;11(1). htttps://doi.org/10.32792/utq/utjsci/v11i1.1151.
12) Hassan AA, Wahid SNA, Hamood HY. Numerical modeling of passively Q-switched Nd: YAG lasers with Cr+4: YAG as a saturable absorber. *Journal of Xidian University*. 2021;15(2). htttps://doi.org/10.37896/jxu15.2/005.
13) Tang J, Bai Z, Zhang D, Yaoyao, Ding J, Wang Y, et al. Advances in All-Solid-State Passively Q-Switched Lasers Based on Cr4+:YAG Saturable Absorber. *Photonics*. 2021;8:93. htttps://doi.org/10.3390/photonics8040093.
14) Gürel Ö. Development of a UV Source Based on Frequency Quadrupling of a Q-switched Nd:YAG Laser. 2009. Available from: https://www.academia.edu/111261631/.
15) Bai Y. Pumping wavelength related population inversion in Nd:doped laser. *AIP Advances*. 2020;10(10):1–6. htttps://doi.org/10.1063/5.0006436.
16) Li M, Qin Y, Wang C, Liu X, Long S, Tang X, et al. Nonuniform pumped passively Q-switched laser using Nd:YAG/Cr4+:YAG composite crystal with high-pulse energy. *Optical Engineering*. 2019;58(3):036106. htttps://doi.org/10.1117/1.OE.58.3.036106.
17) Al-Zurkany SAHS. A Theoretical Study of Optimizing Parameters to Generate Dual Pulses of Passive Q-switching Laser. 2024. Available from: https://dspace.utq.edu.iq/items/5bb46f34-1d48-4c89-b22b-c4ac4db842b2/full.
18) Hussein T, Salih A. Investigation of Effective Beam Area Ratio Effect on Characteristics of Passive Q-Switched Fiber Doped Laser. *Journal of Optoelectronics Laser*. 2022;41(10). htttps://doi.org/10050086.2022.10.47.
19) Tanaka H, Krankel C, Kannari F. Transition-metal-doped saturable absorbers for passive Q-switching of visible lasers. *Optical Materials Express*. 2020;10(8). htttps://doi.org/10.1364/OME.395893.
20) Vp A, Weigand R, Sánchez-Balmaseda M, Pérez JMG. Powerful algebraic model to design Q-switched lasers using saturable absorbers. *Optics and Laser Technology*. 2023;164:1–13. htttps://doi.org/10.1016/j.optlastec.2023.109506.
21) Hussein ZA, Salih AKM. Saturable Absorbent Initial Transmission Effect on Characteristics of Passive Q-switching Er+3 Doped Fiber Laser. *AIP Conference Proceedings*. 2022;2386:080010. htttps://doi.org/10.1063/5.0067126.
22) Tang J, Bai Z, Zhang D, Qi Y, Ding J, Wang Y. Advances in All-Solid-State Passively Q-Switched Lasers Based on Cr+4:YAG Saturable Absorber. *Photonics*. 2021;8(4):1–14. htttps://doi.org/10.3390/photonics8040093.
23) Wang P, Zhu C. Passively Q-Switched and Mode-Locked Fiber Laser Based on a Zeolitic Imidazolate Framework-67 Saturable Absorber. *Frontiers in Physics*. 2022;10:1–8. htttps://doi.org/10.3389/fphy.2022.926344.
24) Koechner W. Solid-State Laser Engineering. Springer. 2013. Available from: https://www.scrip.org.